Macromolecular Research, Vol. 17, No. 6, pp 403-410 (2009)

Albumin-conjugated Cadmium Sulfide Nanoparticles and their Interaction with KB Cells

K. M. Kamruzzaman Selim and Inn-Kyu Kang*

Department of Polymer Science, Kyungpook National University, Daegu 702-701, Korea

Haiqing Guo

College of Chemistry and Molecular Engineering, Peking University, Beijing-100871, China

Received April 25, 2008; Revised October 24, 2008; Accepted November 17, 2008

Abstract: Cytotoxicity is a severe problem of cadmium sulfide nanoparticles (CSNPs) for use in biological systems. In the present study, mercaptoacetic acid-coated CSNPs were conjugated with bovine serum albumin (BSA) to improve biocompatibility. The surface properties of the CSNPs and albumin-conjugated CSNPs (ACSNPs) were characterized by XRD, UV, FTIR, EA, TEM and DLS. Human breast cancer cells (KB cells) were then cultured in the presence of the nanoparticles to evaluate the cytotoxicity of CSNPs and ACSNPs. Finally, the fluorescence intensity of the nanoparticles' aqueous solution was examined using a fluorescence spectrometer. The results showed that the cell compatibility and fluorescence intensity of ACSNPs were higher than those of CSNPs. The strongly luminescent features of the biocompatible ACSNPs are promising for use in biological fields such as cellular labeling, intracellular tracking and molecular imaging.

Keywords: cadmium sulfide nanoparticles, bovine serum albumin, biocompatibility, fluorescence intensity.

Introduction

Semiconductor nanocrystals, known as quantum dots (Q-dots), have got enormous interest in recent time due to their unusual optical and electronic properties. The optical properties of Q-dots depend strongly on their size and composition of their core, which can be controlled by the duration, temperature and the surface capping molecules during their synthesis.[1] Compared with traditional organic fluorophores, Q-dots show considerable advantages including size-tunable emission, narrow spectral line widths, high luminescence, continuous absorption profile and excellent stability against photobleaching. Furthermore, the high surface area to volume ratio of Q-dots makes them appealing for the design of more complex nanosystem.[2] Recent research has shown that Q-dots (CdS, CdSe, CdTe etc.) can be linked with biorecognition molecules such as peptides, antibodies, nucleic acids and small molecules for use as a fluorescent probes.[3] Biological molecules can be fluorescence labeled by attaching Q-dots either by functionalizing biological molecules with a chemical group which is reactive towards the surface of Q-dots[4,5] or by linking biological molecules covalently to the outer hydrophilic shell of Q-dots which bear reactive groups, such as -COOH, -NH_2 or -SH.[6]

*Corresponding Author. E-mail: ikkang@knu.ac.kr

So far, numerous modifications of the Q-dots surface chemistry have been explored, including the attachment of organic layers of poly(ethylene glycol) (PEG),[7] mercaptoacetic acid,[8,9] mercaptopropionic acid,[10] mercaptobenzoic acid[11] and biocompatible and chemically functionalizable inorganic shells such as silica or zinc sulfide.[7] All these coatings can mainly ensure the water solubility of Q-dots and are unable to enhance the biocompatibility considerably. In fact, these coatings alone are insufficient to stabilize the core of Q-dots, particularly, in biological solutions.[12] So further coating with suitable water soluble organic ligand/biomolecules is necessary to enhance the biocompatibility of Q-dots considerably. BSA is a appropriate coating material for conjugation with Q-dots to enhance biocompatibility as well as fluorescence intensity. Besides, BSA-conjugation serves the dual purposes of stabilizing the Q-dots to prevent agglomeration in aqueous suspension and introducing biocompatible functionalities into the Q-dots for further biological interactions or couplings (antibody attachment, for example).[13] Recently, few researchers had conjugated BSA on the surface of Q-dots.[13-18] But most of these reports highlight about the synthesis procedure of BSA-coated Q-dots and the optical behavior of Q-dots after modification by BSA. Very few reports were published showing the optical behavior and the cytotoxicity of Q-dots simultaneously after modification by BSA.

In the current study, mercaptoacetic acid-coated cadmium

sulfide nanoparticles (CSNPs), typical semiconductor Q-dots, were synthesized in an aqueous medium by the arrested precipitation method at room temperature. Then, bovine serum albumin (BSA) was immobilized on the surface of the CSNPs (ACSNPs) to enhance the biocompatibility and fluorescence intensity. The surface properties of CSNPs and ACSNPs were characterized by X-ray diffraction (XRD), UV-vis spectrophotometer (UV-vis), transmission electron microscopy (TEM), dynamic light scaterring (DLS), fourier transform infrared (FTIR) and elemental analysis (EA). Finally toxicity and fluorescence intensity of CSNPs and ACSNPs were evaluated by some cell culture related experiments and fluorescence spectroscopy, respectively.

Experimental

Materials. Cadmium chloride ($CdCl_2$. $2.5H_2O$ > 98%), sodium sulfide (Na_2S. $9H_2O$, 98.0%) and mercaptoacetic acid ($HS\text{-}CH_2COOH$) were purchased from Sigma-Aldrich Co. (USA). Ethylenediamine was purchased from Duksan Pharmaceuticals Co. Ltd (Korea). Bovine serum albumin (BSA) was purchased from Aldrich Chemical Co. (USA). 3-(4,5-Dimethylazol-2-yl)-2,5-diphenyl-2H-tetrazolium bromide (MTT)) was purchased from Sigma Co. (USA). All other chemicals used in this study were analytical grade and used without further purification.

Synthesis of Water Soluble CSNPs. Water soluble CSNPs were synthesized using the previously published method.[9] Briefly, carboxyl-stabilized CSNPs were synthesized by arrested precipitation at room temperature in an aqueous solution using mercaptoacetic acid as the colloidal stabilizer. Nanocrystals were prepared from a stirred solution of 0.0456 g $CdCl_2$ (5 mM) in 40 mL of pure water. The pH was lowered to 2 with mercaptoacetic acid and then raised to 7 with concentrated NaOH. The mixture was deaerated by N_2 bubbling for about 30 min and then, a freshly prepared 40 mL of 5 mM Na_2S (0.0480 g Na_2S in 40 mL water) was added to the mixture with rapid stirring. The solution turned yellow shortly after the sulfide addition due to the cadmium sulfide nanoparticles formation (CSNPs) (reaction scheme is shown in Figure 1(a)). CSNPs were separated from reaction byproducts (sodium salt) by precipitation with the addition of acetone (4 mL of acetone/mL of nanocrystal solution).[7] The precipitate was isolated by centrifugation and dried in a freeze dryer. The prepared powder CSNPs are redispersible in water, whereby a clear colloidal solution is obtained. The free carboxylic acid groups of the prepared CSNPs are suitable for covalent coupling to various biomolecules by covalent interaction to reactive amine groups.

Conjugation of CSNPs with Albumin. Conjugation of CSNPs with albumin involves two steps. First, CSNPs were reacted with ethylenediamine to introduce amine groups on the surfaces. To do so, CSNPs (0.3 g) were dissolved in an aqueous solution (20 mL) containing 1-ethyl-3-(3-dimethylaminopropyl)-carbodiimide hydrochloride (EDC, 4 mg/mL) and stirred for 4 h to activate the carboxylic acid groups on the surfaces. Then, the excess amount of ethylenediamine was added to the solution and stirred for 24 h to obtain primary amine-grafted CSNPs (ECSNPs). To keep free amine groups at one end of the ethylenediamine after the reaction, an excessive amount of ethylenediamine was used in the coupling reaction.[19] The prepared ECSNPs were isolated via repeated centrifugation and finally dried in a freeze dryer.[8] In the second step, albumin was immobilized on the surfaces of ECSNPs as follows: albumin (0.2 g) was dissolved in a phosphate buffer solution (40 mL, pH 7) containing 1-ethyl-3-(3-dimethylaminopropyl) carbodiimide hydrochloride (EDC) and stirred for 5 h to activate the carboxylic acid groups of albumin. Then, ECSNPs (0.3 g) were added to this solution and the mixture was stirred for 48 h at room temperature to obtain albumin-coated ECSNPs (ACSNPs) (reaction scheme is shown in Figure 1(b)). ACSNPs were isolated by repeated centrifugation and stored in phosphate buffered saline (PBS) at pH 7.[8] All the conjugation reactions, unless otherwise noted, were carried out in the dark under a N_2 ambient environment.

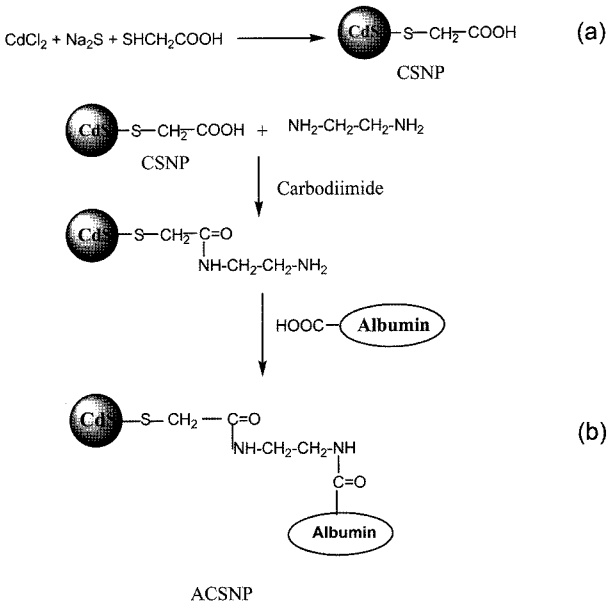

Figure 1. Schematic diagram showing the synthesis of (a) CSNPs and (b) ACSNPs.

Surface Characterization. Fourier transform infrared (FTIR) spectra were obtained using a Jasco, FT-IR 300E spectrometer with a resolution of 4 cm^{-1}. Dried samples were ground with KBr powder and compressed into pellets for FTIR examination. Transmission electron microphotographs (PHILIPS, CM 200 TEM, applied operation voltage; 120 kV) were used to observe the morphology of nanoparticles. To obtain the samples for TEM observations, particles were diluted with distilled water and then deposited on

Formvar-coated 400 mesh copper grids. After drying the nanoparticles fluids thin films on the copper grid, a thin layer of carbon films of about 10-30 nm in thickness was deposited on the nanoparticles fluids film. The hydrodynamic diameter and size distribution were determined by dynamic light scattering (DLS) by means of a standard laboratory-built light scattering spectrometer using a BI 90 particle sizer (Brookhaven Instruments Corp., Holtsville, NY). It had a vertically polarized incident light of 514.5 nm supplied by an argon ion laser (Lexel laser, model 95). The UV-vis absorption spectrum was recorded from aqueous dispersions at room temperature using a Hitachi U-3000 Spectrophotometer. To investigate the crystal structure of CSNPs, X-ray diffraction (XRD, Enraf Nonius, RA/FR-571) was used. The result was compared with JCPDS file no. 10-454 to confirm whether any impurity phase exists in CSNPs. Elemental analysis (EA) was done to confirm the chemical compostion of CSNPs, ECSNPs and ACSNPs by Eager 200 method using CE instrument.

Cell Culture. Human breast cancer cells (KB cells) were used in this experiment. Cells were routinely cultured at 37 °C in a humidified atmosphere with 5% CO_2 (in air), in a 75 cm^2 flask containing 10 mL of RPMI-1640 medium, supplemented with 10% fetal bovine serum (FBS) and 1% penicillin striptomicin G sodium (PGS). Media was changed every third day. For subculture, the cells were washed twice with PBS and incubated with trypsin-EDTA solution (0.25% trypsin, 1 mM EDTA) for 10 min at 37 °C to detach the cells and complete media were then added in the flask at room temperature to inhibit the effect of trypsin. The cells were washed twice by centrifugation and resuspended in the complete media for reseeding and growing in new culture flasks. Cell viability was determined through staining with trypan blue and cells were counted using a hemocytometer. Cell density was estimated using a 0.9 mm^3 counting chamber.

Evaluation of Cytotoxicity. The proliferation of KB cells in a media containing CSNPs and ACSNPs were determined using the MTT (3-{4,5-dimethylthiazol-2yl}-2,5-diphenyltetrazolium bromide) assay. The mechanism behind this assay is that the reduction of the tetrazolium salt into a blue color product (formazan) only occurs in metabolically active cells. The amount of formazan produced is proportional to the number of living cells.[20] Briefly, KB cells were seeded (1×10^5 cell/mL) on 24 well plates in the presence of a cell culture medium. After 24 h, the culture medium was replaced with a fresh medium containing CSNPs and ACSNPs at a particle concentration of 0.2 mg/mL. After being incubated for 1, 2, 3, 4 days, a 50 μL MTT solution (5 mg/mL in PBS) was added to each well and incubated in a humidified atmosphere of 5% CO_2 at 37 °C for 4 h. After removing the medium, the converted dye was dissolved in acidic isopropanol (0.04 N HCl-isopropanol) and kept for 30 min in the dark at room temperature. From each sample, the medium (100 μL) was taken and transferred to a 96-well plate and subjected to ultraviolet measurements for converted dye. This was done at a wavelength of 570 nm on a kinetic microplate reader (EL × 800, Bio-T® Instruments, Inc, Highland Park, USA). The experiment was repeated three times.

Fluorescence Intensity Measurement. Sepectrofluorimetric measurements were carried out on SPEX Fluorolog-2 spectrofluorimeter equipped with a 450W xenon lamp. The fluorescence intensities of solutions were obtained using 1 cm quartz cells. The excitation and emission monochromators were fixed with 0.25 mm slits. Fluorescence was collected and detected by photomultiplier tube (Hamamatsu Model R 928) powered at 950V. All spectral data were obtained by SPEX DM 3000F spectroscopy computer. Origin version 6.0 professional software was used for data processing. For the measurement of the fluorescence spectra, the freeze dried particles (CSNPs and ACSNPs) were dispersed in deionized water (2×10^{-4} g/mL). The fluorescence intensity was measured at 560 nm (excitation at 401 nm) at room temperature.

Statistical Analysis. The cell proliferation experiment was performed in triplicate and the results were expressed as mean ± standard deviation (SD). The student's t test was employed to assess statistical significant difference of the results. Difference was considered statistically significant at $p<0.05$.

Results and Discussion

Surface Characterization. The X-ray diffraction spectrum of CSNPs is shown in Figure 2. It was compared with the data of the JCPDS file no. 10-454 and is in good agreement with that of pure cubic-phase cadmium sulfide, without signals from $CdCl_2$, NaOH and other precursor compounds. The three peaks observed in Figure 2 at 2θ values of 26.439°, 43.862° and 51.389° correspond to the three crystal planes of (111), (220) and (311), indicating that CSNPs are in a cubic phase.[21] Again, the diffraction peaks of CSNPs

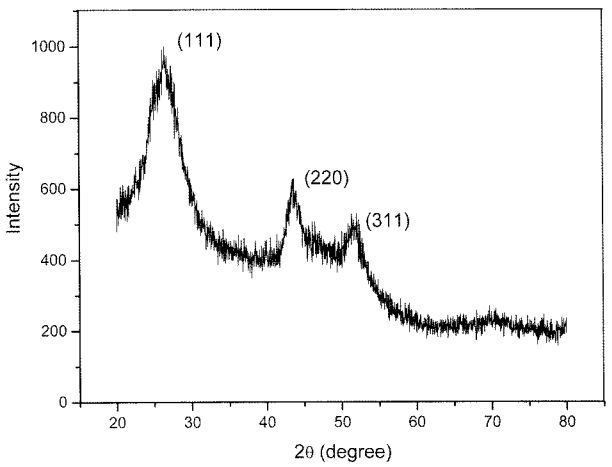

Figure 2. XRD pattern of CSNPs.

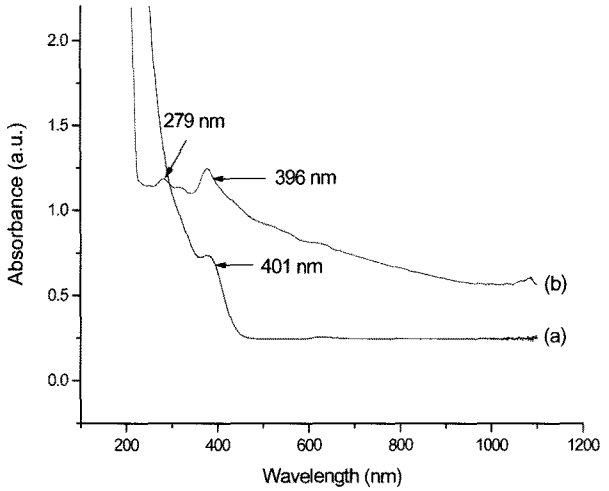

Figure 3. UV-vis spectra of (a) CSNPs and (b) ACSNPs.

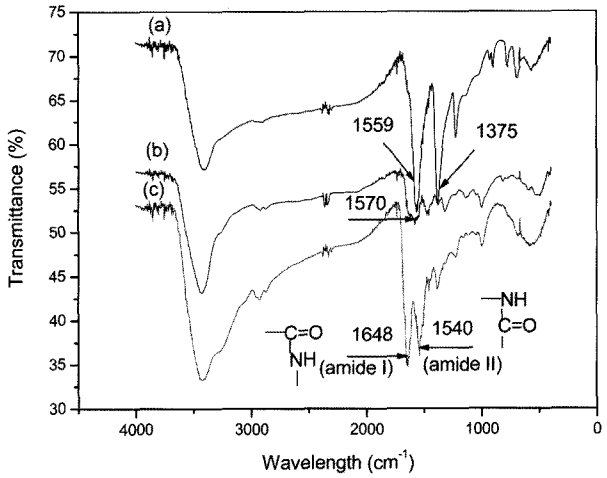

Figure 4. FTIR spectra of (a) CSNPs, (b) ECSNPs, and (c) ACSNPs.

are somewhat broadened. The broadness of the peaks is due to the reduced particle size and surface defects.[22] The small-sized CSNPs possess higher surface defect density due to high surface-to-volume ratio and more Cd atoms with dangling bonds on their surfaces.[23]

Synthesis of cadmium sulfide was further confirmed by UV-vis absorption spectrum as shown in Figure 3(a). CSNPs sample showed an absorption onset at 401 nm and exhibited a blue shift compared to 512 nm for bulk cadmium sulfide.[24] This blue shift was caused by strong quantum confinement, due to the decrease in particle size.[25] On the contrary, Figure 3(b) shows the absorbance of ACSNPs. The main absorption peak of ACSNPs exhibited at 396 nm. In addition, a new band at ca. 279 nm also appeared, which attributed to the BSA labels on the surface of CSNPs. Compared with CSNPs (Figure 3(a)), the absorption band of ACSNPs (Figure 3(b)) did not shift significantly after BSA conjugation (peak position still remains blue shift region). N. Zhu *et al.*[26] conjugated DNA capped cadmium sulfide nanoparticles and showed that main absorption peak did not change significantly after modification and also exhibited a new peak at *ca* 268 nm for DNA capping. UV-vis spectra of this study also showed similar results.

The surface modification of CSNPs with BSA was confirmed by FTIR as displayed in Figure 4. For CSNPs (Figure 4(a)), two distinctive bands were observed at 1559 and 1375 cm^{-1}. This is due to C-O antisymmetric stretching and C-O symmetric stretching bands of acetate ion (-COO-), respectively which clearly indicate the formation of co-ordinate bond between the oxygen atom of mercaptoacetic acid and Cd^{+2}. No free carboxyl acid band at 1800-1740 cm^{-1} due to the C=O stretching band is observed in the capped nanoparticles indicating the formation of co-ordinate bond between Cd^{+2} and oxygen atom.[17,27] In the case of ECSNPs spectrum, the introduction of ethylenediamine on the surface of CSNPs was confirmed by the characteristic peak at 1570 cm^{-1} as shown in Figure 4(b), which attributed to free amine (-NH_2) groups. Again, after reaction of ethylenediamine-coated CSNPs (ECSNPs) with BSA, two new peaks at positions around 1648 and 1540 cm^{-1} were observed in the spectrum of ACSNPs (Figure 4(c)) which are assined to -CO-NH- (amide I) and -CO-NH- (amide II) bonds, respectively.[28] This is because, after the reaction of free amine groups of ECSNPs with BSA, the absorption at 1648 and 1540 cm^{-1} appeared based on amide bonds between carboxylic acid of BSA and amine groups of ECSNPs. These phenomena indicate that BSA was successfully immobilized on the surface of CSNPs.

Immobilization of BSA on the surface of CSNPs was further confirmed by EA. The chemical composition of CSNPs, ECSNPs and ACSNPs are shown in Table I. Carbon content (25.01%) and hydrogen content (6.70%) of ECSNPs were higher than that for CSNPs (carbon content 8.166% and hydrogen content 0.89%). Again, ECSNPs content high percent of nitrogen (17.33%) compared to CSNPs (nitrogen content 0.1002%). The percent of nitrogen CSNPs content is negligible (0.1002%). This negligible amount of nitrogen perhaps exists in CSNPs as experiment was carried out under nitrogen environment or due to the influence of other environmental factors. All these phenomena indicate that ethylenediamine was successfully conjugated on the surface of CSNPs. Again, in the case of ACSNPs, carbon content increased from 25.58 to 32.97%, nitrogen content increased

Table I. Atomic Percent of CSNPs, ECSNPs and ACSNPs Calculated by EA

Sample	Atomic Percent (%)				
	C	H	N	S	O
CSNP	8.1664	0.8943	0.1002	20.2899	13.1102
ECSNP	25.0160	6.7025	17.3373	7.0023	10.2435
ACSNP	32.9765	8.4191	25.5889	2.6799	21.3015

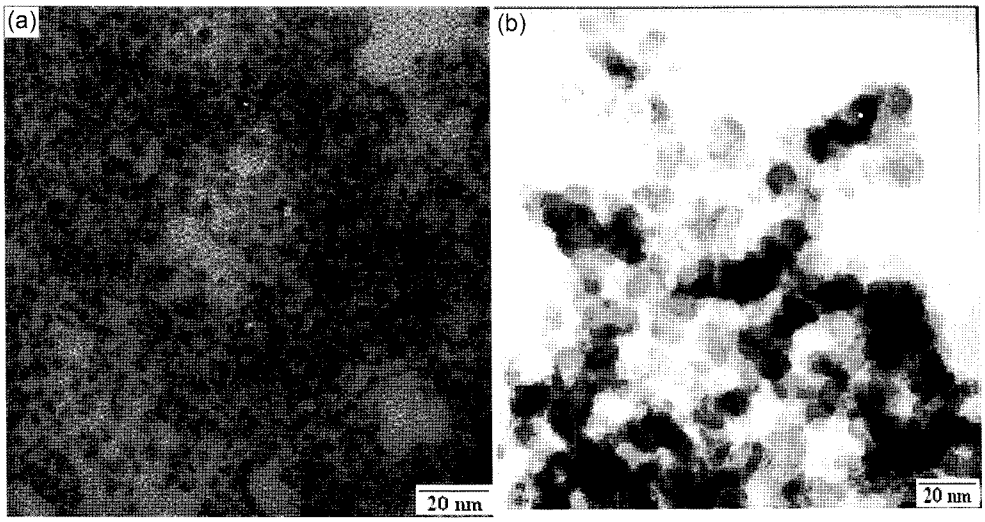

Figure 5. TEM images of (a) CSNPs and (b) ACSNPs.

from 17.33 to 25.58% and oxygen content increased from 10.24 to 21.30%, indicating the successfully immobilization of BSA on the surface of ECSNPs.

The TEM images of CSNPs and ACSNPs are shown in Figures 5(a) and 5(b), respectively. It is observed that CSNPs have a spherical morphology with an average diameter of *ca.* 4.5 nm. Because of the small dimensions and high surface energy of the particles, it is easy for them to aggregate as seen in Figure 5(a). On the other hand, the particles are shaped spherically and comparatively low aggregated particles morphologies having an average particle size of 12 nm are observed in the case of ACSNPs (Figure 5(b)). This larger particles size and non-aggregated particles morphological phenomena may have happened due to the attachment of BSA on the surface of CSNPs.

Figure 6 shows the typical size and size distribution of synthesized CSNPs (Figure 6(a)) and ACSNPs (Figure 6(b)) measured by DLS. The average size of CSNPs as determined by DLS is *ca* 21 nm. On the other hand, average size of the ACSNPs is about 35 nm. The size of the particles as determined by DLS is considerably larger than that determined by TEM. This is because the DLS technique gives a mean hydrodynamic diameter of CSNPs core surrounded by the organic and solvation layers and this hydrodynamic diameter is influenced by the viscosity and the concentration of the solution.[29,30] On the other hand, TEM gives the diameter of the core alone. Again, CSNPs are highly monodisperse as shown in Figure 6(a). In contrast, ACSNPs (Figure 6(b)) are far more polydisperse.[31]

Cytotoxicity. Figure 7 shows the phase contrast light microscope photographs (×200) of KB cells (Figure 7(a)), after a 72 h culture in a media containing ACSNPs (Figure 7(b))

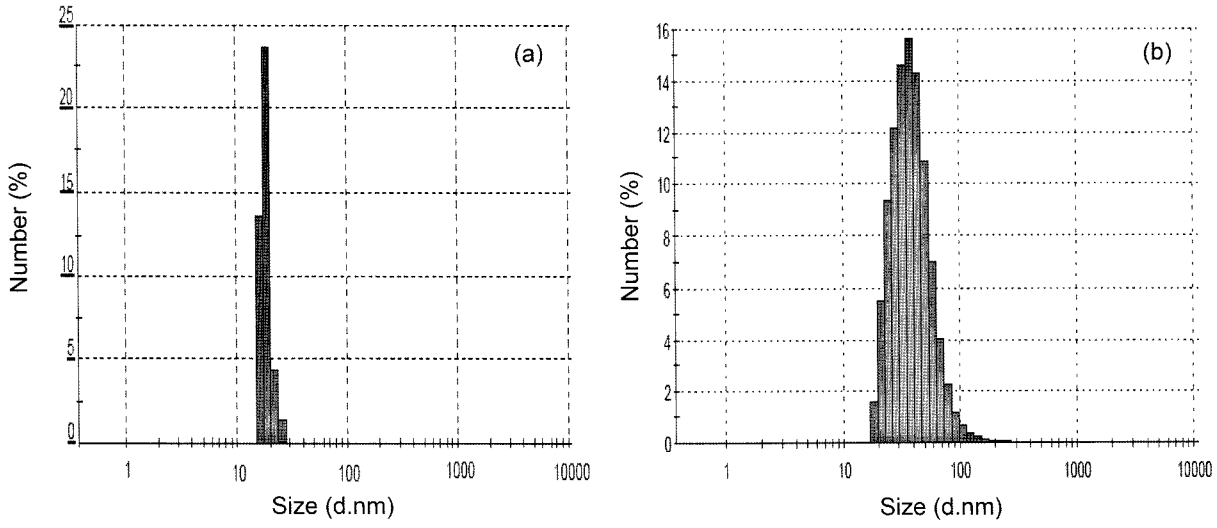

Figure 6. Particle size distribution of (a) CSNPs and (b) ACSNPs measured by DLS.

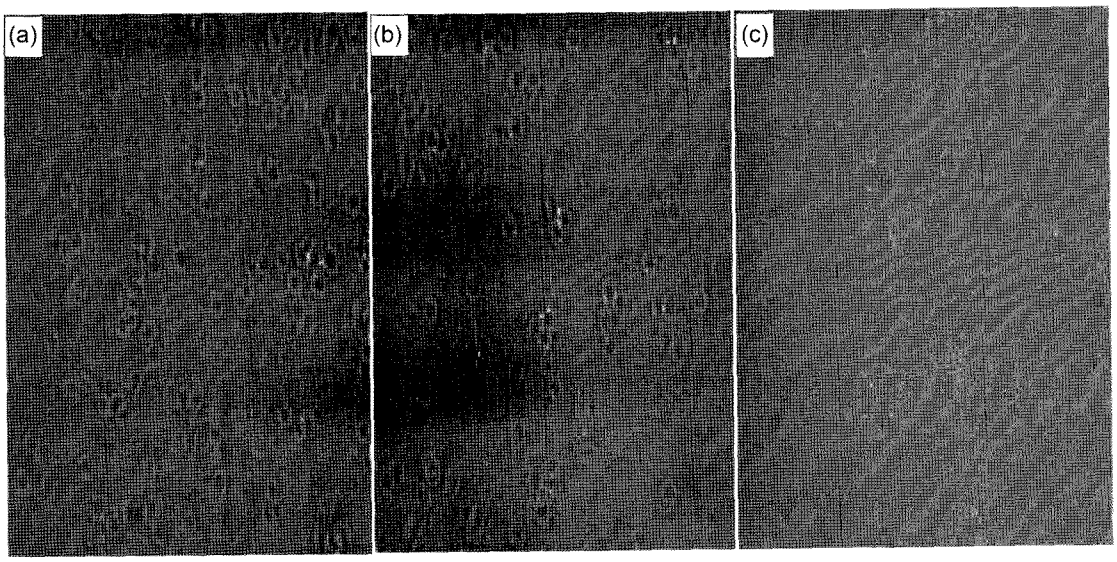

Figure 7. Phase contrast photographs of (a) KB cells control culture, (b) cells after 72 h of growth in a media containing ACSNPs and (c) CSNPs.

and CSNPs (Figure 7(c)). The morphology of the cells after a 72 h incubation with ACSNPs was close to that of the control cells (KB cells), suggesting good biocompatibility of ACSNPs over the time frame. On the other hand, most of the cells died after a 72 h culture with CSNPs and the remaining cells membranes were also distorted as shown in Figure 7(c). Cells death might have happened due to (i) release of interior cadmium ion (Cd^{+2}) from CSNPs into the cell media and cause the cells death and/or (ii) formation of reactive oxygen species (ROS).[32] Releasing of cadmium ion from CSNPs into cell media is due to the surface oxidation of CSNPs.[33,34] It has been postulated that chalcogenide atoms (Se, S) located on the surface of the Q-dots could be oxidized by oxygen molecules to form oxides (SeO_2, SO_4^{2-}).[34]

$$CdS+O_2 \xrightarrow{h\nu} Cd^{2+}+SO_4^{2-}$$

In the case of CSNPs, the formed SO_4^{2-} molecules release from the surface, leaving behind "dangling" reduced Cd atoms. Thus, prolonged exposure of CSNPs to an oxidative environment can cause the decomposition of CSNPs, thereby leading to release of Cd ion. On the contrary, in the case of ACSNPs, surface ligand (BSA) decreases the Q-dots surface oxidation by reducing transport of oxygen to the surface. Again, Q-dots are redox active nanoparticles (effective electron donors and acceptors)[35] and can generate highly reactive free radicals with or without exposure to light.[36] Q-dots can induce ROS generation through energy or electron transfer to molecular oxygen.[36,37] Cells respond to even small changes of intracellular redox status which is sufficient to inhibit proliferation and induce differentiation.[38] So protection of the Q-dots surface plays a crucial role. Particles with surfaces well protected by polymers or proteins are mostly not harmful to cells whereas breaking down of protective coating leads to cell damage and death.[32] In the present study, mercaptoacetic acid and BSA were used as coating materials for cadmium sulfide nanoparticles. Mercaptoacetic acid is one of the smallest solubilization ligands and thus the least protective of the Q-dots surface.[33] So, this coating fails to bar the diffusion of cadmium for a longer period. On the other hand, BSA coating perhaps reduced the surface oxidation and barred the diffusion of Cd^{+2}, resulting the enhanced biocompatibility.[33]

The cells proliferation in a media treated with CSNPs and ACSNPs at days 1, 2, 3, 4 were analyzed by MTT assay as shown in Figure 8. From the very first day of culture, the proliferation rate with ACSNPs was higher than that with CSNPs with standard deviation. However, after a culture of

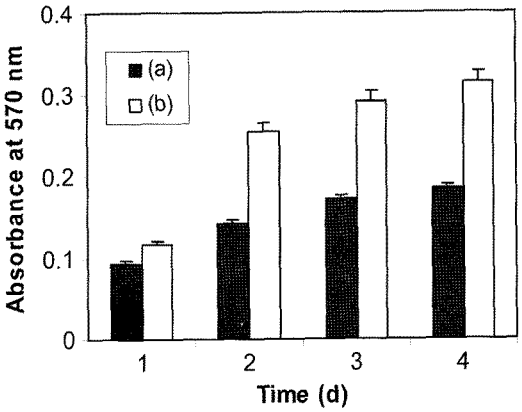

Figure 8. Viability of KB cells in the presence of (a) CSNPs and (b) ACSNPs measured by MTT assay. (Data are expressed as mean ± SD (n=3) for the specific absorbance).

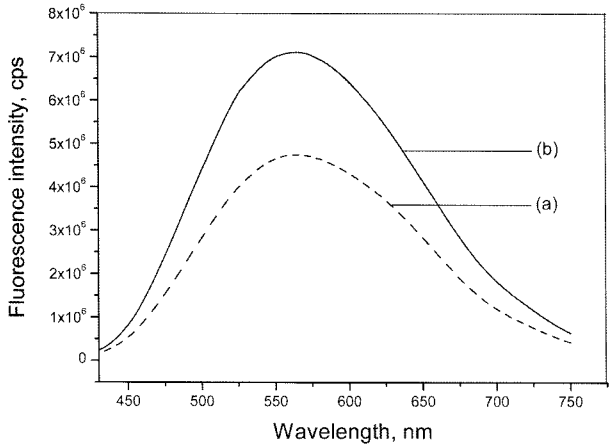

Figure 9. Fluorescence spectra (λ_{ex}=401 nm) of (a) CSNPs and (b) ACSNPs. The measured aqueous solutions have the same concentrations.

2, 3 and 4 days cell proliferation rate with ACSNPs increased significantly (P<0.05) compared to that with CSNPs. In other words, it can be stated that the surface modification of cadmium sulfide with BSA could lessen the cytotoxicity of cadmium sulfide considerably in comparison to that modified by mercaptoacetic acid.

Fluorescence Intensity. The fluorescence spectra (excitation at 401 nm) of CSNPs and ACSNPs were shown in Figure 9. It is interesting to note that the fluorescence intensity of ACSNPs (Figure 9(b)) increased significantly compared to CSNPs (Figure 9(a)) at the same concentration. It was demonstrated that the fluorescence intensity of ACSNPs was stronger by *ca* 1.5-fold than that for CSNPs. This result coincides with the results reported by Kuo *et al.*[17] and Wang *et al.*.[23] In their reports, they conjugated BSA with cadmium telluride (CdTe) and consequently showed the enhancement of fluorescence intensity after modification by BSA. The reasons for this increased fluorescence quantum yield may be: (a) firstly, though the -COOH of mercaptoacetic acid linked to the cadmium sulfide surface, there might still be many defects on the surface. When BSA was conjugated with CSNPs, BSA could modify the defects on the surface of CSNPs and thus minimized the number of surface defects, resulting in enhancement of the fluorescence intensity,[18] (b) secondly, the formation of a few double- and triple-dot aggregates induced by the conjugation of BSA,[39] and (c) finally, the resonance energy transfer from the tryptophan moieties in BSA to the CSNPs.[13] Compared with CSNPs, enhanced fluorescence labeled ACSNPs are more stable (at least 2 months) in aqueous solution at 4 °C. The fluorescence of ACSNPs remains almost constant in phosphate buffer (pH 7.4) at ionic strengths up to 400 mM and it is possible to introduce biocompatible functionalities into ACSNPs for further biological interactions or couplings (antibody attachment, for example).

Conclusions

Mercaptoacetic acid-coated cadmium sulfide nanoparticles (CSNPs) were successfully conjugated with bovine serum albumin. The albumin-conjugated CSNPs (ACSNPs) showed considerably low cytotoxicity compared to CSNPs. ACSNPs also exhibited stronger fluorescence intensities than the non-conjugated CSNPs. Highly fluorescence labeled and enhanced biocompatible ACSNPs could be used in many biological applications such as *in vitro* or *in vivo* cell imaging and analytical purposes.

Acknowledgment. This work was supported by a grant from the Advanced Medical Technology Cluster for Diagnosis and Prediction at KNU from MOCIE, Republic of Korea.

References

(1) L. Chen, J. Zhu, Q. Li, S. Chen, and Y. Wang, *Eur. Polym. J.*, **43**, 4593 (2007).
(2) Z. Li, K. Wang, W. Tan, J. Li, Z. Fu, C. Ma, H. Li, X. He, and J. Liu, *Anal. Biochem.*, **354**, 169 (2006).
(3) A. M. Smith, X. Gao, and S. Nie, *Photochem. Photobiol.*, **80**, 377 (2004).
(4) W. J. Parak, T. Pellegrino, and C. Plank, *Nanotechnology*, **16**, 9 (2005).
(5) M. E. Akerman, W. C. W. Chan, P. Laakkonen, S. N. Bhatia, and E. Ruoslahti, *Proc. Natl. Acad. Sci. USA*, **99**, 12617 (2002).
(6) K. I. Hanaki, A. Momo, T. Oku, A. Komoto, S. Maenosono, Y. Yamaguchi, and K. Yamamoto, *Biochem. Biophys. Res. Commun.*, **302**, 496 (2003).
(7) N. Gomez, J. O. Winter, F. Shieh, A. E. Saunders, B. A. Korgel, and C. E. Schmidt, *Talanta*, **67**, 462 (2005).
(8) W. C. W. Chan and S. Nie, *Science*, **281**, 2016 (1998).
(9) H. M. Chen, X. F. Huang, L. Xu, J. Xu, K. J. Chen, and D. Feng, *Superlatt. Microstruc.*, **27**, 1 (2000).
(10) G. P. Mitchell, C. A. Mirkin, and R. L. Letsinger, *J. Am. Chem. Soc.*, **121**, 8122 (1999).
(11) C. C. Chen, C. P. Yet, H. N. Wang, and C. Y. Chao, *Langmuir*, **15**, 6845 (1999).
(12) T. Jamieson, R. Bakhshi, D. Petrova, R. Pocock, M. Imani, and A. M. Seifalian, *Biomaterials*, **28**, 4717 (2007).
(13) M. J. Meziani, P. Pathak, B. A. Harruff, R. Hurezeanu, and Y. P. Sun, *Langmuir*, **21**, 2008 (2005).
(14) S. Nayar, A. Sinha, S. Das, S. K. Das, and P. R. Rao, *J. Mater. Sci. Lett.*, **20**, 2099 (2001).
(15) J. G Liang, X. P. Ai, Z. K He, H. Y Xie, and D. W Pang, *Mater. Lett.*, **59**, 2778 (2005).
(16) L. Y. Wang, Y. Y. Zhou, L. Wang, C. Q. Zhu, Y. X. Li, and F. Gao, *Anal. Chem. Acta*, **466**, 87 (2002).
(17) Y. C. Kuo, Q. Wang, C. Ruengruglikit, H. Yu, and Q. Huang, *J. Phys. Chem. C*, **112**, 4818 (2008).
(18) C. Jiang, S. Xu, D. Yang, F. Zhang, and W. Wang, *Luminescence*, **22**, 430 (2007).
(19) J. S. Bae, E. J. Seo, and I. K. Kang, *Biomaterials*, **20**, 529 (1999).
(20) K. S. Chow, E. Khor, and A. C. A. Wan, *J. Polym. Res.*, **8**, 27

(2001).
(21) N. V. Smith, *X-Ray Powder Data Files*, American Society for Testing and Materials, Philadelphia, 1967.
(22) A. Pucci, M. Boccia, F. Galembeck, C. A. P. Leite, N. Tirelli, and G. Ruggeri, *Reactive & Functional Polym.*, **68**, 1144 (2008).
(23) Q. Wang, Y. C. Kuo, Y. Wang, G. Shin, C. Ruengruglikit, and Q. Huang, *J. Phys. Chem. B*, **110**, 16860 (2006).
(24) A. L. Pan, J. G. Ma, X. Z. Yan, and B. S. Zou, *J. Phys. Condens. Matter.*, **16**, 3229 (2004).
(25) L. E. Brus, *J. Chem. Phys.*, **80**, 4403 (1984).
(26) N. Zhu, A. Zhang, P. He, and Y. Fang, *Analyst*, **128**, 260 (2003).
(27) P. S. Chowdhury, P. Ghosh, and A. Patra, *J. Lumines.*, **124**, 327 (2007).
(28) I. K. Kang, B. K. Kwon, J. H. Lee, and H. B. Lee, *Biomaterials*, **14**, 787 (1993).
(29) K. M. K. Selim, J. H. Lee, S. J. Kim, Z. Xing, Y. Chang, H. Guo, and I. K. Kang, *Macromol. Res.*, **14**, 646 (2006).
(30) Y. L. Wu, C. S. Lim, S. Fu, A. I. Y. Tok, H. M. Lau, F. Y. C. Boey, and X. T. Zeng, *Nanotechnology*, **18**, 1 (2007).
(31) A. S. Blum, C. M. Soto, C. D. Wilson, J. L. Whitley, M. H. Moore, K. E. Sapsford, T. Lin, A. Chatterji, J. E. Johnson, and B. R. Ratna, *Nanotechnology*, **17**, 5073 (2006).
(32) D. Maysinger, J. Lovric, A. Eisenberg, and R. Savic, *Eur. J. Pharm. Biopharm.*, **65**, 270 (2007).
(33) A. M. Derfus, W. C. W. Chan, and S. N. Bhatia, *Nano Lett.*, **4**, 11 (2004).
(34) L. Spanhel, M. Haase, H. Weller, and A. Henglein, *J. Am. Chem. Soc.*, **109**, 5649 (1987).
(35) S. K. Haram, B. M. Quinn, and A. J. Bard, *J. Am. Chem. Soc.*, **123**, 8860 (2001).
(36) J. Lovric, S. J. Cho, F. M. Winnik, and D. Maysinger, *Chem. Biol.*, **12**, 1227 (2005).
(37) A. C. Samia, X. Chen, and C. Burda, *J. Am. Chem. Soc.*, **125**, 15736 (2003).
(38) M. Noble, M. Mayer-Proschel, and C. Proschel, *Antioxid. Redox Signal*, **7**, 1456 (2005).
(39) C. W. Liua and H. T. Chang, *Open. Anal. Chem. J.*, **1**, 1 (2007).